Journal of Drug Delivery Science and Technology 84 (2023) 104443

Contents lists available at ScienceDirect

Journal of Drug Delivery Science and Technology

journal homepage: www.elsevier.com/locate/jddst

Encapsulation of carvacrol and thymol for a persistent removal of *Listeria innocua* biofilms

Jina Yammine [a,b], Adem Gharsallaoui [c], Alexandre Fadel [d], Layal Karam [e], Ali Ismail [b], Nour-Eddine Chihib [a,*]

[a] Univ Lille, CNRS, INRAE, Centrale Lille, UMR 8207 – UMET – Unité Matériaux et Transformations, Lille, France
[b] Plateforme de Recherches et D'Analyses en Sciences de L'Environnement (PRASE), Ecole Doctorale des Sciences et Technologies, Université Libanaise, Hadath, Lebanon
[c] Univ Lyon, Université Claude Bernard Lyon 1, CNRS, LAGEPP UMR, 5007, Villeurbanne, France
[d] Univ Lille, CNRS, INRAE, ENSCL, Université D'Artois, FR 2638, IMEC – Institut Michel-Eugène Chevreul, F-59000, Lille, France
[e] Human Nutrition Department, College of Health Sciences, QU Health, Qatar University, Doha, Qatar

ARTICLE INFO

Keywords:
Carvacrol
Thymol
Nanoencapsulation
Sustained release
Biofilms
Listeria innocua

ABSTRACT

Chemical disinfectants along with various mechanical methods are still commonly used in the food industry to disinfect food contact surfaces. A new strategy that could replace them is by encapsulating carvacrol (CAR) and thymol (THY) in monolayer (ML) and layer-by-layer (LBL) nanocapsules. ML nanocapsules were developed using a single carrier material maltodextrin, whereas pectin was additionally added to the LBL nanocapsules. Physicochemical characterizations (size, charge, polydispersity index) and microscopy observations of nanocapsules revealed increased size and thickness of the wall shell with the additional layer in the LBL nanocapsules. The release kinetics of CAR and THY over a 20 h period fitted into the Korsmeyer-Peppas model and followed a Fickian release behavior combining dissolution and diffusion. ML nanocapsules revealed an initial burst release of terpenes with 90.52% released during the first 2 h, followed by a steady release phase. Whereas, only up to 50.71% of terpenes were released from the LBL nanocapsules during the first 2 h, with a progressive continuous release over time until reaching up to 95.68% after 20 h. The activity against *Listeria innocua* biofilms was consistent with the release curves of CAR and THY. A successive exposure of biofilms to ML followed by LBL nanocapsules ensured a 99.99% inhibition of biofilms for up to 6 h. It is thus confirmed that a successive application of nanocapsules is a promising strategy to ensure a long-term protection of food contact surfaces.

1. Introduction

Foodborne illnesses and outbreaks are increasingly attracting global attention. Among the major foodborne pathogens, *Listeria monocytogenes* is able to survive under acidic conditions and refrigeration temperatures, making it a pathogen of serious concerns in the food processing industry. *L. monocytogenes* is a Gram-positive bacterium that can be found in food and in processing areas. This psychrophilic bacterium is also capable of adhering to surface equipment like stainless steel, rubber or glass [1]. One of the main concerns facing the food industry remains in the persistence of pathogens on surfaces and their subsequent contamination and formation of complex biofilm structures [2,3]. Biofilms are a community of bacterial cells adsorbed on a surface and embedded within an extrapolymeric matrix that provides protection from various environmental factors [4]. As a result, bacterial cells acquire increased resistance to stress conditions and disinfectants compared to their planktonic counterparts [5,6]. In 2020, the European Food Safety Authority (EFSA) and the European Center for Disease Prevention and Control (ECDC), reported that *L. monocytogenes* was involved in the most severe zoonotic diseases with the highest number of fatalities (13%) [7]. In this study, the non-pathogenic *L. innocua* was used instead of the pathogenic *L. monocytogenes* due to the considerations of containment and as previous works suggested that *L. innocua* may surrogate *L. monocytogenes* as they react similarly in biofilm formation and chemical and physical treatments [8–10]. *L. innocua* is a rod-shaped Gram-positive bacterium commonly found in the same processing environments or foods as *L. monocytogenes* [11]. It is mobile, non-hemolytic, and can grow at temperatures as low as 4 °C posing a threat to the food industry [12].

To control biofilms, environmentally-friendly biologically based

* Corresponding author. Certia Inrae, 369 rue Jules Guesde, 59650, Villeneuve d'Ascq, France.
E-mail address: nour-eddine.chihib@univ-lille.fr (N.-E. Chihib).

https://doi.org/10.1016/j.jddst.2023.104443
Received 23 November 2022; Received in revised form 30 March 2023; Accepted 9 April 2023
Available online 10 April 2023
1773-2247/

antimicrobial agents such as carvacrol (CAR) and thymol (THY) have been emphasized as effective alternatives to chemical disinfectants [13,14]. CAR and THY are two geometric isomers, phenolic monoterpenoids found as major constituents in the essential oils (EOs) of various plants, especially oregano, thyme, wild bergamot, and pepperwort [15]. An extensive literature has been reported about their potent antibiofilm activities against several microorganisms such as *Salmonella* sp., *Staphylococcus aureus*, and *Pseudomonas aeruginosa* [16–19].

However, the use of EOs in their free forms remains a major limitation for the food industry. Therefore, successful encapsulation techniques have been widely used to entrap EOs and increase their stability, reduce their volatility, and improve their water solubility by preserving and protecting them from environmental conditions [20]. Encapsulation could also ensure a controlled and sustained release of EOs, widely spreading their various applications, and in particular their extended disinfection effect with better protection of surfaces from a potential risk of recontamination [21].

Therefore, two types of nanocapsules encapsulating CAR and THY were developed and characterized in this study. The *in vitro* mechanisms and kinetics of release of CAR and THY from both types of capsules were studied and determined by different mathematical models. Furthermore, the antibiofilm activity of ML and LBL nanocapsules, applied alone or in a sequential treatment, was evaluated against *L. innocua* biofilms developed on stainless steel surfaces over time. This was performed to clarify the effect of the sustained release properties of the capsules for long-lasting disinfection of food contact surfaces.

2. Materials and methods

2.1. Chemicals and antimicrobial agents

CAR (98% purity) and THY (≥99% purity) were purchased from Sigma-Aldrich (St. Louis, MO, USA). For the formation of ML capsules, maltodextrins DE 21 (MD) purchased from Roquette-Frères SA (Lestrem, France) were used as the carrier material. For LBL capsules, low-methoxyl pectin (LMP) from Cargill (Baupte, France) was added as a second layer. Sodium caseinate (CAS) powder from Thermo Fisher Scientific (United Kingdom) was used as an emulsifier for both types of capsules. A neutralizing solution containing Tween 80 (30 g L^{-1}), Sodium Thiosulphate (5 g L^{-1}), Saponin (30 g L^{-1}), Tryptone salt (TS) broth (9.5 g L^{-1}), L-Histidine (1 g L^{-1}), and Lecithin (30 g L^{-1}) was used to stop the antimicrobial activity of the various antimicrobial solutions used for biofilm treatment.

2.2. Monolayer and layer-by-layer nanocapsules formation

The two types of capsules encapsulating CAR and THY were developed using the spray-drying technique. Spray-drying is a cost-effective technique in which different parameters can be controlled to achieve the desired properties of the final product [22]. In addition, it ensures high retention of the encapsulated materials and produces low-moisture particles in powder form, which facilitates handling [23]. ML nanocapsules were developed using MD, a natural polysaccharide, as a carrier material combined with CAS, an animal-based protein, as an emulsifier. For the formation of LBL nanocapsules, an additional LMP polysaccharide carrier layer was added to MD and CAS. For both types of nanocapsules, primary emulsions were prepared by complete hydration of CAS in distilled water at room temperature. The pH of the emulsion was adjusted to 3 by adding HCl or NaOH (0.1 or 1.0 M). Weighted amounts of CAR and THY were then added to the stock solutions and homogenized using an Ultra Turrax PT 4000 homogenizer (Polytron, Kinematica, Switzerland) operating at 20 000 rpm for 5 min. The homogenized emulsions were further microfluidized at 500 bar and five recirculation using an LM20 Microfluidizer (Microfluidics Co., MA, USA). For subsequent preparation of ML-CAR and ML-THY, stock solutions of MD (50% w/v) were added to the emulsions to obtain final compositions (w/w) of: 20.0% MD, 0.5% CAS and 1.0% CAR or 1.0% THY. For the formation of LBL-CAR and LBL-THY, previously prepared LMP stock solutions and MD solutions (50.0% w/v) were added to the primary emulsions to obtain final compositions (w/w) of: 20.0% MD, 0.5% CAS, 0.5% LMP and 1.0% CAR or 1.0% THY. The pH of the final solutions was adjusted to 3 before the spray-drying process. The feed emulsions were continuously stirred and then injected into a 0.5 mm nozzle of the drying chamber of a laboratory spray-dryer (Mini Spray-Dryer Büchi B-290, Switzerland). The operating conditions for the drying process were previously optimized to the following parameters: 180 ± 2 °C air inlet temperature, 80 ± 5 °C air outlet temperature, 0.5 L h^{-1} feed flow rate and 3.2 bar for air pressure. The collected powder particles were separated from the cyclone and stored in sealed containers at 4 °C until further analysis.

2.3. Characterization of the encapsulated oily droplets and capsules

The size, polydispersity index (PDI) and electrical charge known as zeta potential (ζ-Potential) of the encapsulated oily droplets were assessed using a Zetasizer Nano ZS90 (Malvern Instruments, Malvern, United Kingdom). One gram of the prepared dried capsules was suspended in 50 mL imidazole-acetate buffer with a pH of 3 and gently shaken. All measurements were made in triplicate, and average sizes were expressed in nanometers (nm), while ζ-Potential values were expressed in millivolts (mV).

Moreover, the internal and external morphology of the spray-dried capsules were examined using scanning electron microscopy (SEM) facility of the Advanced Characterization Platform of the Chevreul Institute (SEM; model JSM-7800FLV, JEOL, Japan) with a scanning voltage of 3 kV. For the inner observations, a layer of powder particles was crushed with a razor blade, while for the outer observations, powder particles were used directly without crushing them. A thin layer of the prepared powders was spread and fixed on a double-sided adhesive tape (Agar scientific, Oxford) mounted on a specimen stub. Prior to microscopic observations, the samples were sputter-coated with a carbon layer using a precision etching coating system (PECS; Gatan 682) to achieve electrical conductivity.

2.4. In vitro release profile of carvacrol and thymol from nanocapsules

The *in vitro* release profile of CAR and THY from nanocapsules prepared with different wall materials was performed according to previous studies [24–28] with slight modifications. The nanocapsules were suspended at 10 mg/mL in a phosphate buffer saline solution (PBS, pH 7.0) with constant stirring at room temperature. The suspensions were then transferred to a dialysis bag (Molecular Weight cut-off of 3500 Da, Thermo Fisher Scientific, United Kingdom) permeable to CAR and THY (MW < 200 Da) but not to MD, CAS or LMP (MW > ≈ 20 kDa) and their nanoparticles [24]. The bag was sealed and then immersed in 25 mL of PBS solution (pH 7.0) with gentle magnetic stirring at room temperature. The release assays of CAR or THY were carried out at preset time intervals (7 min, 15 min, 30 min, 1 h, 1 h 30 min, 2 h and then until reaching 20 h), by withdrawing aliquots of 3 mL from the outer phase of the dialysis bags and replacing it with an equivalent volume of fresh PBS solution to maintain a constant total volume. The amounts of CAR and THY released were determined by measuring the absorption intensity with a UV–visible spectrophotometer (SAFAS UVmc2, Monaco) at a wavelength of 275 nm and 277 nm, the maximum absorbance of CAR and THY, respectively, in a neutral solution. The amounts of CAR and THY released were then calculated using previously generated standard calibration curves: Absorbance = 0.2173 x + 0.0709; R^2 = 0.9991, and Absorbance = 0.2238 x + 0.0744; R^2 = 0.9993, for free CAR and THY, respectively. Tests were performed in triplicate and the cumulative release percentages of CAR and THY from the nanocapsules were calculated using the following equation:

$$Cumulative\ release\ (\%) = \sum_{t=0}^{t}\left(\frac{Q_t}{Q_0}\right) \text{x } 100$$

where Q_t is the cumulative amount of CAR or THY released at each sampling time t, and Q_0 is the initial amount of CAR or THY loaded in the samples.

2.5. Mathematical modelling of carvacrol and thymol release

In order to explain the release mechanism of CAR and THY from both types of nanocapsules, the release data were fitted to different mathematical kinetic models that best describe the release of components from polymeric delivery systems [29]. Mathematical models have become important tools to predict and generalize the experimental data [30,31]. As a result, experimental data can be adjusted to optimize release conditions and minimize the number of experiments [32]. The used mathematical models were: (1) zero-order, (2) first-order, (3) Higuchi and (4) Korsmeyer-Peppas kinetics based on the following equations:

$$Q_t = Q_0 + K_0 t \quad (1)$$

$$\ln Q_t = \ln Q_0 + K_1 t \quad (2)$$

$$Q_t = K_H\, t^{0.5} \quad (3)$$

$$Q_t = K_{KP} t^n \quad (4)$$

where Q_t is the cumulative amount of CAR or THY released at time t, Q_0 is the initial amount of CAR or THY loaded into the nanocapsules, K_0, K_1, K_H, K_{KP}, are the release rate constants for the zero order, first order, Higuchi and Korsmeyer-Peppas models, respectively. n in equation (4) represents the release exponent that indicates the release mechanism of CAR and THY. If $n \leq 0.43$, it corresponds to a Fickian mechanism combining dissolution and diffusion, $0.43 < n < 0.85$ represents a non-Fickian transport combining diffusion and swelling mechanisms, $n = 0.85$ corresponds to a zero-order release model and $n > 0.85$ represents a super case- II transport [33]. Correlation coefficients (R^2) were calculated for each model. K constants and n values were determined by estimation using Microsoft Excel 2021.

2.6. Determination of the minimal inhibitory concentrations (MIC) against L. innocua planktonic cells

Experiments were carried out on *L. innocua* (ATCC 33090) strains grown overnight in Tryptic Soy Broth (TSB; Biokar Diagnostics, Pantin, France) until mid-exponential phase was reached. Bacterial cells were then harvested by centrifugation at 5000 rpm for 5 min at 20 °C and washed twice with Potassium Phosphate Buffer (PPB; 100 mM, pH 7.0). For MIC determination, 100 µL of 10^6 CFU mL^{-1} bacterial suspensions were added to the wells of a microtiter plate assay containing 100 µL of Müller-Hinton broth (MHB; Biokar Diagnostics, Pantin, France) and 100 µL serial two-fold dilutions of ML and LBL capsules to yield final concentrations ranging from 0.156 to 10 mg mL^{-1}. For positive control wells, bacterial suspensions were added to MHB without the antimicrobials tested. MHB was used alone as negative control. Microdilution plates were then incubated at 37 °C with a continuous agitation in a Bioscreen C (Labsystems, Helsinki, Finland) and optical density at 600 nm (OD_{600}) was measured every 2 h for 24 h. MIC values were determined as the lowest concentration of an antimicrobial agent that prevents the visible growth of bacteria. All tests were performed in triplicate using different microplates.

2.7. Time-kill curve assay

The bactericidal activity of ML and LBL nanocapsules was tested using the plate colony counting method. Briefly, overnight cultures of *L. innocua* were used to prepare a cell suspension with a final concentration of 10^6 CFU mL^{-1}. The bacterial suspensions were then exposed to the different antimicrobial solutions previously prepared in MHB based on their MIC values and kept under constant shaking. At different time intervals: 1 min, 5 min, 30 min, and 1 h to 8 h after inoculation, cultures were plated onto Mueller Hinton agar (MHA, Difco Pont-de-Claix, France) at an appropriate dilution. Subsequently, colony counting was performed after incubation for 24 h at 37 °C. Control sets were similarly performed without the antimicrobial agents. All tests were performed at least three times.

2.8. Antibiofilm assays

2.8.1. Biofilms formation

Stainless steel (SS) slides (INOX 304L, Equinox, France) 1 mm thick and 41 mm in diameter were previously sterilized with ethanol and autoclaved at 121 °C for 20 min. Subsequently, the sterile slides were placed in the reactor chambers of the NEC biofilm system as previously described by Ref. [34]. Three mL of 10^7 CFU mL^{-1} *L. innocua* cell suspensions were deposited on the slides and allowed to adhere for 1 h at 20 °C. The slides were then rinsed with 5 mL of PPB to remove non-adherent cells and covered with 3 mL of TSB and incubated at 37 °C for 24 h to allow biofilm formation. Biofilms were then rinsed with PPB and used for the various antimicrobial treatments.

2.8.2. Exposure of biofilms to encapsulated carvacrol and thymol

To determine if there was a relationship between antibiofilm activity and the cumulative amounts of CAR and THY released from the nanocapsules, SS slides with biofilms developed overnight were immersed in 3 mL of the different antimicrobial solutions (ML-CAR, ML-THY, LBL-CAR, and LBL-THY) prepared in TS broth according to their ½ MIC values. The antibiofilm activity of the ML and LBL capsules was recorded over several exposure times (30 min, 1 h, 2 h, 3 h, 4 h, 5 h and 6 h). In a second part, to evaluate the efficacy of initial use of ML nanocapsules to reduce biofilms, followed by application of LBL nanocapsules to provide prolonged antibiofilm activity and surface protection, *L. innocua* biofilms were sequentially exposed to ½ MIC of the ML capsules for 30 min followed by direct exposure to the LBL capsules for the same previous exposure times. After immersion in the various antimicrobial solutions, for the specific treatment time, the slides were removed and immersed in 5 mL of neutralizing solution for 10 min. Then, for detachment and quantification of bacterial cells, the slides were transferred to 20 mL TS broth, vortexed for 30 s, and sonicated at 37 kHz for 5 min (Elmasonic S60H, Elma, Germany). Detached cells were plated on Tryptic Soy Agar (TSA; Biokar Diagnostics, France) and counted after 24 h incubation at 37 °C. Results were then expressed as log CFU cm^{-2}. For control assays, slides were immersed in TS broth. Results represent the mean values of three independent experiments, using two slides for each experiments.

2.9. Scanning electron microscopy observations for L. innocua biofilms

The morphology of the untreated control bacterial cells and those exposed to the MIC of the different antimicrobial agents for 15 min was assessed using the scanning electron microscopy (SEM). Treated and untreated bacteria recovered from the biofilms were serially diluted tenfold in TS broth, and 1 mL of the suspension was filtered using a 0.2 µm polycarbonate membrane filter (Schleicher & Schuell, Dassel, Germany). The filter was then immersed in cacodylate buffer (0.1 M; pH 7.0) containing 2% glutaraldehyde for 4 h at 4 °C. The fixed samples were then dehydrated in graded ethanol series for 10 min at each concentration (50, 70, 95 and twice 100% (v/v)), critical point dried and further coated with a thin layer of carbon prior to SEM observations.

2.10. Statistical analysis

Experiments were performed in triplicate, and results were expressed

as mean ± standard deviation (S.D.). Statistical analysis was performed by the Analysis of variance (ANOVA) followed by Tukey's test using Matplotlib software (Version 3.3.4., Python). Significance between the means of the results was determined at $p < 0.05$.

3. Results and discussion

3.1. Characteristics of the encapsulated droplets and the developed nanoparticles

The average size, PDI and ζ-Potential values of the encapsulated droplets are shown in Table 1. The sizes reported for the ML droplet emulsions were significantly different from those of the LBL emulsions ($p < 0.05$). The size differences could be attributed to the additional layer of pectin carrier material in the formulation of LBL emulsions. Pectin may contribute to a higher viscosity of the emulsions and thus an increase in their size [35]. The PDI values of all droplets were less than 0.3, indicating a uniform size distribution of the droplets in the formulations [36]. On the other hand, the ζ-Potential values determined for the ML droplet emulsions were positive due to the positively charged CAS at pH 3 below its isoelectric point (pHi ~ 4.5). In the LBL emulsions, there was a transition to negative ζ-Potential values, which could be due to the presence of negative carboxyl groups on the surface of the added pectin [35]. Pectin with low degree of esterification, as used in this study (LMP), has a higher amount of negative charges that allow easier formation of bonds and thus better contact with CAS chains [35]. The negatively charged pectin polymers in LBL emulsions cause more pronounced electrostatic attraction with the positively charged CAS. This explains why the absolute ζ-Potential values of the LBL emulsions were lower than those measured for the ML emulsions. The lower ζ-Potential values and stronger interparticle attraction reported for the LBL emulsions reduce the stability of the particles. Nevertheless, the stability is not only dictated by ζ-Potential values, but could also be related to other factors such as size, viscosity, and density of the emulsions.

As shown in Fig. 1, SEM microscopic images of the external morphology of most types of dried capsules revealed well-defined spherical capsules with a smooth surface. Some of the capsules showed little evidence of cracks on their external surfaces, probably due to the slow diffusion of water during the spray-drying process [37]. As for the internal morphologies, the capsules exhibited a shell structure with voids in the center. A thicker shell layer was observed in the internal structure of the LBL capsules (Fig. 1) g), and 1) h)) which could be related to the additional presence of pectin that increases the thickness of the shell.

3.2. Sustained release profile of carvacrol and thymol from capsules

CAR and THY *in vitro* release profile was assessed to understand the release kinetics from capsules prepared with different carrier materials. The release kinetics were studied in a PBS solution with a pH 7.0, and the results are shown in Fig. 2. As can be seen, the concentrations of CAR and THY released over 20 h were dependent on the type of capsule, which can be attributed to the different compositions of the carrier materials and their subsequent efficient retentions. The release of CAR and THY from the ML nanocapsules was characterized by an initial rapid release followed by a sustained slower release of terpenes over 20 h. The initial phase of rapid release occurred during the first 7 min after resuspension of the ML nanocapsules in a PBS solution, with 65.67% and 55.09% of CAR and THY released, respectively. Thus, more than 50% of the encapsulated agents were released from the ML nanocapsules in the first 7 min. Analogous results were reported by Ref. [38]; who showed that most of the microencapsulated *Mentha spicata* EO was released in the first 7 min. This initial phase of release lasted for up to 2 h for the ML nanocapsules, with 90.52% and 82.55% of CAR and THY released, respectively. The rapid release phase from the ML nanocapsules could be ascribed to the hydrophilicity of the MD carrier polymers, which leads to rapid hydration of the capsules once they are suspended in PBS solution, resulting in rapid diffusion of the encapsulated agents [37,39]. In addition, it is strongly believed that CAR and THY released during this initial stage were located near or adsorbed on the surface of the capsules and have a weak affinity to the carrier materials [26,40]. Two hours after the re-suspension of the ML nanocapsules in the release medium, the release rates of CAR and THY were slowed down and reached a steady state with the highest cumulative release percentages of 96.18% and 93.14% after 20 h, respectively. The subsequent release phase of CAR and THY from the ML nanocapsules was characterized by a slow and sustained release over several hours, which might be mainly due to the longer period required for the diffusion of CAR and THY from the shell coating. In contrast, a different release trend was observed for the LBL nanocapsules, as there was no initial burst release phase, but rather a continuous and progressive release over time. In the first 7 min after re-suspension of the LBL-CAR and LBL-THY nanocapsules in the release medium, the cumulative release percentages were of only 25.97% and 22.03%, respectively. Five hours were required to release 75.96% and 70.18% of the encapsulated CAR and THY, respectively. The results showed that the ML nanocapsules emphasized a superior dissolution behavior compared to the LBL nanocapsules, which allowed faster diffusion of the encapsulated agents. The lower and delayed released amounts of CAR and THY from the LBL nanocapsules during the first hours could be attributed to the presence of the additional pectin layer, which could explain the longer time required for the diffusion of CAR and THY through the capsule shell [41]. In addition, capsules acquire a more compact and dense coating structure when MD and LMP carrier materials are combined, which impedes the release and diffusion of the encapsulated agents. After 5 h, the release rates of CAR and THY from the LBL nanocapsules slowed down but gradually continued to increase, reaching the highest cumulative release percentages of 95.68% and 89.83%, respectively, after 20 h. Our results show that diffusion of the encapsulated CAR and THY from the LBL nanocapsules takes more time due to the thicker and more complex shell coating [42]. After 20 h, the released amounts of CAR and THY from both types of nanocapsules did not reach the initial loaded amounts. For a complete diffusion and release of the encapsulated CAR and THY, further exposure time might be required.

It should also be noted that the release rate of the encapsulated agents depends not only on the carrier materials used, but also on the size and ζ-Potential values, which could play an important role in the release mechanism, as reported by Ref. [43]. A decrease in particle size increases the subsequent release rate of the encapsulated agents due to the larger surface area that exposes more particles to the release medium [24]. ML nanocapsules with small size showed higher release rates of both CAR and THY compared to LBL nanocapsules. In addition, the ζ-Potential results could explain the slower release of CAR and THY from the LBL nanocapsules. The lower ζ-Potential values could lead to stronger aggregation and attraction between the LBL particles. As a result, the surface area of the capsules exposed to the release media is smaller, leading to a lower release of the encapsulated agents [44].

Our results also showed that the release of CAR was higher than that of THY from both types of capsules. This could be explained by the crystallizable nature of the phenols of THY, which could hinder their

Table 1
Average size, polydispersity index (PDI) and zeta potential (ζ-Potential) of carvacrol (CAR) and thymol (THY) droplet emulsions encapsulated in monolayer (ML) and layer-by-layer (LBL) capsules.

Type of Capsule	Size (nm)	PDI	ζ-Potential (mV)
ML-CAR	184.76 ± 7.88	0.27 ± 0.03	24.66 ± 0.90
ML-THY	159.25 ± 7.23	0.23 ± 0.01	23.60 ± 1.35
LBL-CAR	316.09 ± 4.33	0.18 ± 0.02	−6.41 ± 0.33
LBL-THY	283.62 ± 2.47	0.19 ± 0.01	−3.45 ± 0.15

Means ± standard deviations are illustrated in Table 1.

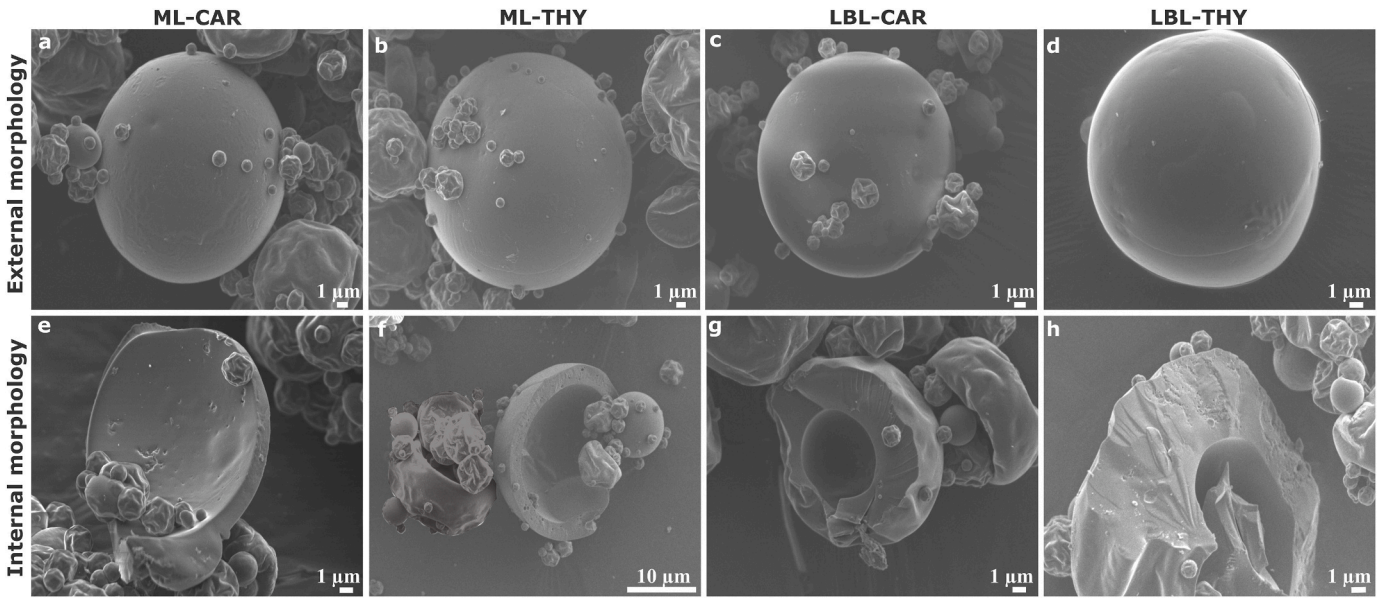

Fig. 1. SEM micrographs of the external structures of a) ML-CAR (4000 ×), b) ML-THY (3300 ×), c) LBL-CAR (4000 ×), d) LBL-THY (5000 ×), and the internal structures of e) ML-CAR (5000 ×), f) ML-THY (2500 ×), g) LBL-CAR (5000 ×), and h) LBL-THY (5000 ×).

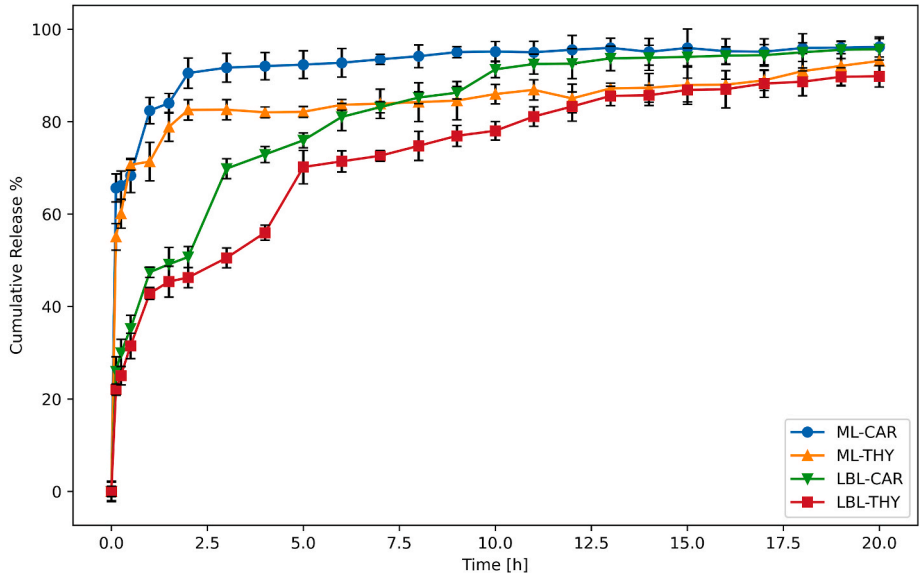

Fig. 2. In vitro cumulative release profile of CAR and THY from ML and LBL nanocapsules in phosphate buffer saline solution (PBS, pH 7.0) at room temperature. Results are expressed as mean ± SD.

diffusion through the shell of the carrier materials [45]. In contrast, CAR in its liquid form could diffuse more easily through the shell. Since CAR is more hydrophilic than thymol due to steric hindrance by the hydroxyl group, a higher release of CAR is expected when the capsules come into contact with a release medium [46].

3.3. Mathematical release kinetics of carvacrol and thymol

To evaluate the mechanism of release of CAR and THY from ML and LBL nanocapsules, the experimental release data were fitted with different kinetic equations such as the zero-order model, the first-order model, the Higuchi model, and the Korsmeyer-Peppas model, which best describe the release of compounds from polymeric carrier systems. Mathematical modelling can help to understand whether or not the release rate depends on the concentration of the compound, or whether the release follows a specific behavior such as diffusion, dissolution, desorption or surface erosion [47]. Understanding the release kinetics of CAR and THY from nanocapsules could help predict their behavior over time and determine what amounts are released at specific time points. For each mathematical model, the constants as well as the correlation coefficients (R^2) and the values of the diffusion exponent n for the Korsmeyer-Peppas model are given in Table 2. The highest R^2 values yielded the best-fitting model for the release mechanism. Analysis of the results revealed that the Korsmeyer-Peppas model best described the release kinetics of CAR and THY from ML and LBL nanocapsules in neutral pH medium, as the reported R^2 values were the highest (0.8800–0.9829). According to this model, the release exponent n could dictate the mechanisms associated with the release of CAR and THY. n should be less than or equal to 0.43 to represent a Fickian mechanism combining diffusion and dissolution, whereas an anomalous mechanism resulting from combined diffusion and swelling mechanisms occurs when n values are between 0.43 and 0.85 [48]. $n = 0.85$ corresponds to a

Table 2
Kinetic parameters of the different mathematical fitting models for the release of carvacrol and thymol from ML and LBL nanocapsules in PBS solution (pH = 7.0).

Model	Zero-order		First-order		Higuchi		Korsmeyer-Peppas		
	K_0	R^2	K_1	R^2	K_H	R^2	K_{KP}	n	R^2
ML-CAR	1.0448	0.5067	0.0126	0.4832	41.2957	0.6992	78.8157	0.0786	0.8800
ML-THY	1.1321	0.6364	0.0146	0.6169	36.7297	0.7841	71.3060	0.0848	0.9168
LBL-CAR	3.0593	0.7549	0.0488	0.6503	33.9703	0.9103	45.9990	0.2739	0.9616
LBL-THY	3.0590	0.8339	0.0540	0.7297	31.3855	0.9553	39.7280	0.2900	0.9829

Abbreviations: ML-CAR: monolayer carvacrol, ML-THY: monolayer thymol, LBL-CAR: layer-by-layer carvacrol, LBL-THY: layer-by-layer thymol.

case II transport dominated by an erosion release mechanism, and a super case-II transport mechanism dominated by relaxation and swelling occurs when $n > 0.85$ [33,49]. The reported low n values ($n \leq 0.43$) suggest that the mechanisms associated with the release of CAR and THY from both types of capsules are dominated by a Fickian mechanism [50]. This mechanism could be explained by the combination of two phenomena: dissolution of carrier materials and diffusion of CAR and THY based on the concentration gradient as reported by Ref. [51]. It can also be noted that the Higuchi model provides a good fit for the release of CAR and THY from the LBL nanocapsules following the Korsmeyer-Peppas model ($R^2 > 0.9$). This confirms that the release trend from the LBL nanocapsules follows a diffusion mechanism as reported by Ref. [52]. Since the R^2 values obtained for the zero and first-order models were lower, it can be concluded that the release rates of CAR and THY were neither constant over time nor proportional to their concentrations [42,52,53]. Thus, it can be confirmed that the release of CAR and THY was mainly controlled by diffusion and dissolution mechanisms. Moreover, K_{KP} diffusion constants were significantly ($p < 0.05$) higher for the ML nanocapsules indicating a higher diffusion rate as compared to the LBL nanocapsules [50]. These results demonstrate facilitated diffusion of CAR and THY from the ML nanocapsules, which are composed of one type of carrier material, compared with the LBL nanocapsules, which provide sustained and prolonged release due to their complex bilayer structure.

3.4. Determination of the minimal inhibitory concentrations of monolayer and layer-by-layer CAR and THY nanocapsules against L. innocua

The MIC of ML and LBL nanocapsules were determined against planktonic cells of *L. innocua*. Regular bacterial growth curves were reported for the control groups. The MIC values determined for ML-CAR and ML-THY nanocapsules against planktonic cells of *L. innocua* were 0.31 and 0.62 mg mL^{-1}, respectively. *L. innocua* was more sensitive to CAR than to THY. For LBL-CAR and LBL-THY, both determined MIC values were reduced by two-folds with values of 0.15 and 0.31 mg mL^{-1}, respectively. The LBL nanocapsules had lower MIC values and thus higher inhibitory activity against *L. innocua* compared to the ML nanocapsules. The lower MIC values of the LBL nanocapsules may be related to the sustained release of terpenes over time, which likely ensures more efficient antimicrobial activity and a longer inhibitory effect on bacterial cells than in the case with the ML nanocapsules, which exhibit a burst inhibition with lower efficiency.

3.5. Assessment of the required time to kill more than 99% of a bacterial population of approximately 6 log

Time-kill assays were performed to investigate the time required to kill more than 99% of an initial *L. innocua* cell suspension of approximately 6 Log when exposed to encapsulated CAR and THY. This is a suitable method to understand the dynamic interaction between the antimicrobials and the exposed microorganisms. The control group without treatment had a bacterial population of approximately 6 log CFU mL^{-1}. The results presented in Fig. 3 show that the ML and LBL nanocapsules were able to exert deleterious effects on *L. innocua* at their MIC values, but at different exposure times. ML-CAR and ML-THY induced a reduction of more than 6 logs (99.99% eradication) of *L. innocua* in 10 and 30 min, respectively. These results highlight the potential of ML nanocapsules to reduce microbial populations in a relatively short time. In another study, reduced microbial growth below the detection limit was observed after a 15 min exposure to encapsulated

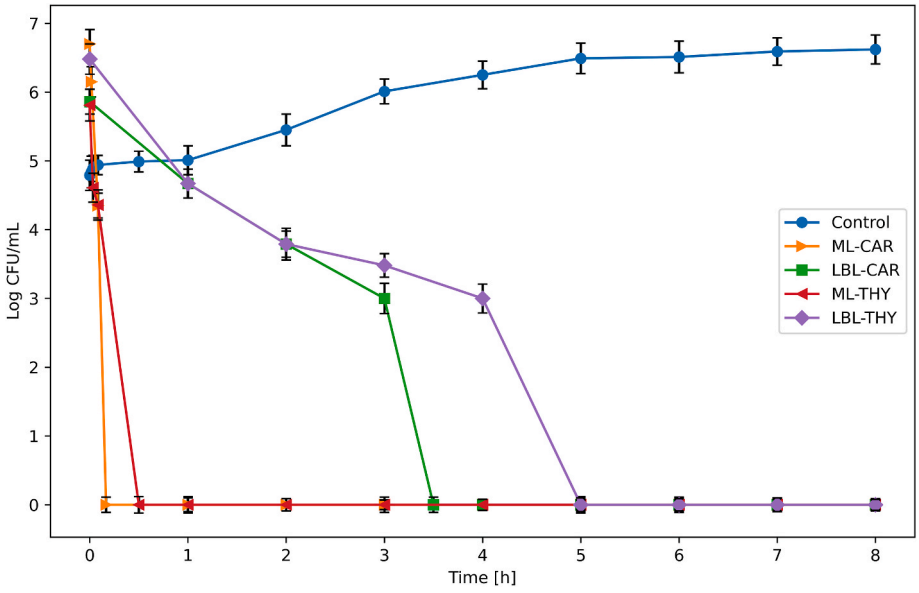

Fig. 3. Time-kill curves of monolayer carvacrol (ML-CAR), monolayer thymol (ML-THY), layer-by-layer carvacrol (LBL-CAR), and layer-by-layer thymol (LBL-THY) nanocapsules against L. innocua planktonic cells.

carvacrol, although the MIC values were higher than those reported in our study [5,6]. This rapid action of ML nanocapsules suggests that CAR and THY may have directly affected bacterial membranes integrity due to the large amounts released. The LBL nanocapsules required longer periods to achieve bactericidal activity against *L. innocua*. For the LBL-CAR and LBL-THY nanocapsules, the cell count progressively decreased within few hours after treatment. More than 6 log reductions in the initial population were observed after 3 h 30 min and 5 h, respectively. At these specific times, approximately 70% of CAR and THY were released from the LBL nanocapsules. The delayed effect could be related to the longer time required for diffusion of CAR and THY through the thick complex structure of the LBL nanocapsules, which consists of two types of carrier materials. The delayed release could slow down the bactericidal effect of the encapsulated agents. This explains why the LBL nanocapsules took up to 5 h to exert a bactericidal effect.

3.6. Antibiofilm activity of carvacrol and thymol nanocapsules

The antibiofilm activities of ML and LBL capsules were evaluated against *L. innocua* biofilms developed on SS after different treatment times (Fig. 4). Exposure of the biofilms to ½ MIC of the capsules not only served to highlight their strong antibiofilm activities, but was also performed to verify the relationship between the cumulative percentages of CAR and THY released from the nanocapsules and their corresponding antibiofilm activities, as higher concentrations could not show this effect (data not shown). The control group showed an initial biofilm count of 7.1 log CFU cm^2 after 24 h of incubation. The applied capsules resulted in a time-dependent reduction of biofilms. After 30 min exposure to ML-CAR and ML-THY, 2.2 and 2.8 log reductions were induced, respectively. For the same exposure time, LBL-CAR and LBL-THY achieved 1.2 and 1.1 log reductions, respectively. Lower and insufficient concentrations of CAR and THY released in the first 30 min (31.50–35.23%) may explain why LBL nanocapsules achieved lower reductions than ML nanocapsules, which released 68.36% and 70.65% of CAR and THY, respectively. The results demonstrate that the additional LMP layer increases the thickness of the core shells of the LBL capsules, resulting in additional protection and slower diffusion of the encapsulated agents with consequent lower antibiofilm efficiency. Additional reductions of 3.2 and 3.1 logs were measured after 1 h exposure to the ML-CAR and ML-THY nanocapsules, respectively. The significant ($p < 0.05$) reductions elicited by ML nanocapsules during the first hour could be explained by the high concentrations of CAR (82.41%) and THY (71.36%) that diffused from the capsules. Nevertheless, after about 2 h of exposure to the ML nanocapsules, no antibiofilm effect was observed anymore, as the reduction of biofilms remained around 3.2–3.4 log until the 6th hour. This could be related to the released amounts of CAR and THY from the ML nanocapsules, which have reached a steady state after 2 h, so no further antibiofilm effect was observed. In contrast, with increasing exposure time, the LBL nanocapsules caused further reductions of *L. innocua* biofilms. In the first 2 h of exposure to the LBL nanocapsules, a reduction of less than 2 log was measured as no more than 50.71% and 46.27% of CAR and THY were released, respectively. The amounts released from the nanocapsules were probably not sufficient to induce higher population reduction. However, after the third hour of exposure to CAR and THY LBL nanocapsules, a progressive increase in the antibiofilm activity was achieved with reductions of 2.64 and 2.20 logs, respectively. Moreover, after 6 h, a reduction in the initial biofilm population of 3.14–3.40 logs was observed. The continuous decrease in bacterial counts over time after treatment with the LBL nanocapsules, is attributed to the sustained diffusion of CAR and THY, which reached 81.03% and 71.42%, respectively after 6 h. This suggests that the antibiofilm activity results are consistent with the release curve trends, as higher antibiofilm activities were reported with higher release rates. Other studies also reported prolonged antimicrobial activity of eugenol-entrapped ethosome nanoparticles against fruit anthracnose due to the slower release over time [54]. In addition, thyme, ginger, and cinnamon EOs encapsulated in chitosan nanoparticles exhibited sustained release over a long period of time, prolonging their antimicrobial activities against *Bacillus subtilis*, *Escherichia coli*, and *Staphylococcus aureus* [55].

3.7. Antibiofilm activity assessment using a successive treatment of monolayer and layer-by-layer nanocapsules

For the second part of the antibiofilm assessment, *L. innocua* biofilms were sequentially exposed to ½ MIC of the ML nanocapsules for 30 min followed by direct exposure to ½ MIC of the LBL nanocapsules for up to 6 h. The sequential treatment was performed to determine the efficacy of the ML nanocapsules for immediate disinfection of SS surfaces following the immediate release of CAR and THY. In addition, the long-term bactericidal activity of the LBL nanocapsules was evaluated against residual surviving bacterial cells not previously eliminated by the ML nanocapsules. The number of bacterial cells encountered by the LBL nanocapsules was already reduced from 7.1 log (control) to 4.9 log and

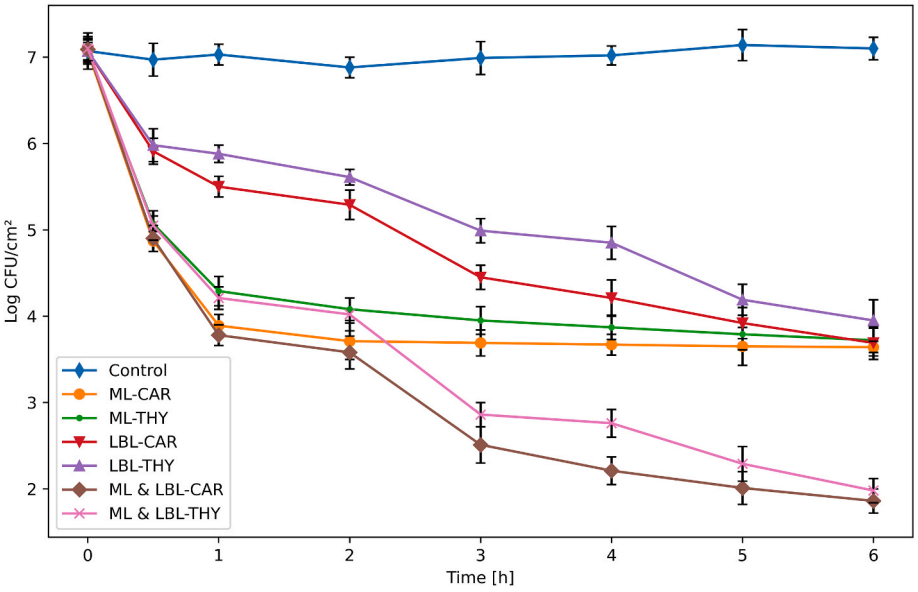

Fig. 4. The antibiofilm activity of ML and LBL nanocapsules applied alone or successively against L. innocua biofilms.

5.1 log after 30 min exposure to ML-CAR and ML-THY, respectively. The LBL nanocapsules were then introduced to achieve a sustained reduction in bacterial counts over a longer period of time. After exposure to the LBL nanocapsules, it is clear from Fig. 4, that bacterial counts continued to decrease over time, until they were eventually undetectable (<2 logs). This resulted in a biofilm bacterial reduction of 99.99% after 6 h. These results confirm that LBL nanocapsules can provide sustained removal of bacterial biofilms and prolonged disinfection efficacy. The progressive release from LBL nanocapsules would protect CAR and THY from the degradative reactions, thus prolonging their antimicrobial efficacy for a longer period of time until release. The results demonstrate that ML nanocapsules could be more effective for initial disinfection of surfaces due to the rapid release of CAR and THY. In contrast, LBL nanocapsules are an important tool to ensure a long-lasting disinfection of surfaces due to their sustained release properties. Sustained disinfection protects surfaces from potential risks of recontamination, and especially during non-operational periods in the food industry.

3.8. Scanning electron microscopy observation of control and treated L. innocua biofilms

The morphologies of the biofilms of control *L. innocua* and those exposed to MIC of ML and LBL CAR and THY nanocapsules were examined using SEM (Fig. 5). The microscopic images of the control biofilms show an intact rod-like structure of *L. innocua* with a relatively smooth surface. No signs of cytolysis were observed on the surface of the untreated bacterial cells. In contrast, after 15 min exposure to the various treatments, the integrity of the bacterial cells decreased, which was clearly evident from the change in shape from rod-shaped structures to irregularly shrunken bacterial cells. According to the literature, CAR and THY have the ability to destabilize bacterial cell membranes and trigger the release of intracellular components [56]. This was confirmed by the SEM observations of the treated cells showing a complete destruction and deformation of the integrity of the bacterial cells. It can also be concluded that the encapsulated CAR and THY had the ability to penetrate the matrix of biofilms and cause the observed morphological changes.

4. Conclusion

A positive relationship was demonstrated between the amounts of CAR and THY released from the nanocapsules and their antibiofilm activities, as higher inhibition of *L. innocua* biofilms was observed at higher release percentages of CAR and THY. The results of this study highlight the potential of successive use of ML nanocapsules followed by LBL nanocapsules, to inhibit biofilms over a longer period of time. ML nanocapsules provided an initial rapid disinfection efficacy over short periods of time, followed by LBL nanocapsules, which offered more benefits for sustained and persistent disinfection of food contact surfaces and provided a long-term efficacy. The LBL nanocapsules provided sustained release of CAR and THY over a 20 h period, which could be proved useful in eliminating residual bacterial biofilms and protecting surfaces from bacterial contamination even during non-operational periods. These results are promising for future applications where the combined antibiofilm effect of both types of capsules can be used for disinfection purposes.

Author statement

Jina Yammine: Writing – Original Draft, Visualization, Investigation, Formal Analysis **Adem Gharsallaoui**: Investigation, Writing – Review & Editing **Alexandre Fadel**: Investigation **Layal Karam**: Conceptualization, Supervision **Ali Ismail**: Validation, Writing – Review & Editing **Nour-Eddine Chihib**: Conceptualization, Writing – Review & Editing, Validation.

Funding

This work was supported by the Partenariat Hubert Curien PHC Cèdre program [Grand number: 42281SD].

Declaration of competing interest

The authors declare that they have no known competing financial interests or personal relationships that could have appeared to influence

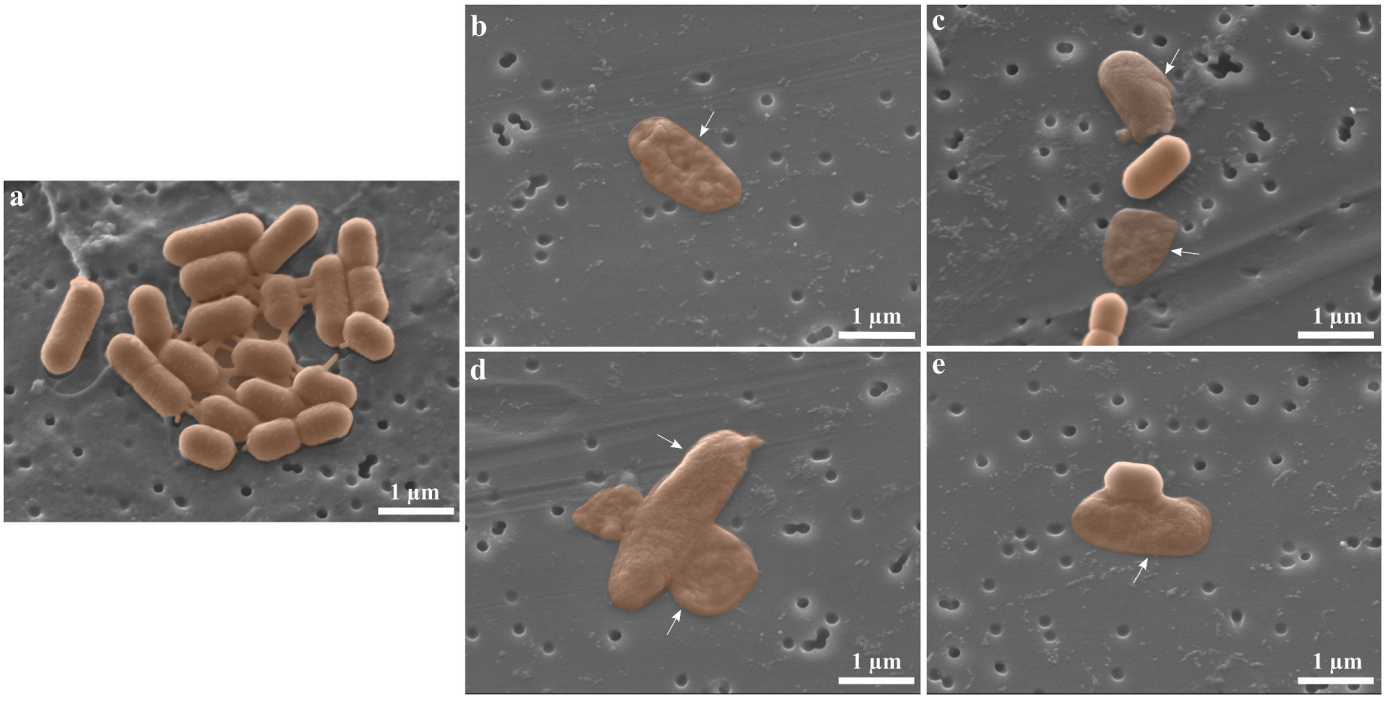

Fig. 5. SEM micrographs of L. innocua biofilms untreated (a), and treated with (b) ML-CAR, (c) LBL-CAR, (d) ML-THY, and (e) LBL-THY (20 000 x). White arrows indicate bacterial cells with morphological alterations.

the work reported in this paper.

Data availability

Data will be made available on request.

Acknowledgements

The Chevreul Institute is thanked for its help in the development of this work through the ARCHI-CM project supported by the “Ministère de l’Enseignement Supérieur de la Recherche et de l’Innovation”, the region “Hauts-de-France”, the ERDF program of the European Union and the “Métropole Européenne de Lille.

References

[1] M. Somrani, H. Debbabi, A. Palop, Antibacterial and antibiofilm activity of essential oil of clove against *Listeria monocytogenes* and *Salmonella* Enteritidis, Food Sci. Technol. Int. 5 (2021) 331–339, https://doi.org/10.1177/10820132211013273.

[2] A.A. Olanbiwoninu, B.M. Popoola, Biofilms and their impact on the food industry, Saudi J. Biol. Sci. 103523 (2023), https://doi.org/10.1016/j.sjbs.2022.103523.

[3] J. Yammine, A. Gharsallaoui, A. Fadel, S. Mechmechani, L. Karam, A. Ismail, N. E. Chihib, Enhanced antimicrobial, antibiofilm and ecotoxic activities of nanoencapsulated carvacrol and thymol as compared to their free counterparts, Food Control 143 (2023), 109317, https://doi.org/10.1016/j.foodcont.2022.109317.

[4] S. Chitlapilly Dass, R. Wang, Biofilm through the looking glass: a microbial food safety perspective, Pathogens 11 (2022), https://doi.org/10.3390/pathogens11030346. Article 346.

[5] S. Mechmechani, A. Gharsallaoui, A. Fadel, K.E. Omari, S. Khelissa, M. Hamze, N. E. Chihib, Microencapsulation of carvacrol as an efficient tool to fight *Pseudomonas aeruginosa* and *Enterococcus faecalis* biofilms, PLoS One 17 (2022), e0270200, https://doi.org/10.1371/journal.pone.0270200.

[6] S. Mechmechani, S. Khelissa, A. Gharsallaoui, K.E. Omari, M. Hamze, N.E. Chihib, Hurdle technology using encapsulated enzymes and essential oils to fight bacterial biofilms, Appl. Microbiol. Biotechnol. 106 (2022) 2311–2335, https://doi.org/10.1007/s00253-022-11875-5.

[7] European Food Safety Authority & European Centre for Disease Prevention and Control, The European union one health 2020 zoonoses report, EFSA J. 19 (2021), https://doi.org/10.2903/j.efsa.2021.6971. Article e06971.

[8] A. Costa, A. Lourenco, T. Civera, L. Brito, *Listeria innocua* and *Listeria monocytogenes* strains from dairy plants behave similarly in biofilm sanitizer testing, Lebensm. Wiss. Technol. 92 (2018) 477–483, https://doi.org/10.1016/j.lwt.2018.02.073.

[9] S. Perni, S.J. Jordan, P.W. Andrew, G. Shama, Biofilm development by *Listeria innocua* in turbulent flow regimes, Food Control 17 (2006) 875–883, https://doi.org/10.1016/j.foodcont.2005.06.002.

[10] M.C.D. Rosa, R. Iacuzio, G.R. Barbosa, R.D.C.L. Pereira, M. Cruzado-Bravo, V.L. M. Rall, D.C. Vallim, N.C.C. Silva, Detection of Listeria innocua in the dairy processing chain: resistance to antibiotics and essential oils, Food Sci. Technol. 42 (2022), https://doi.org/10.1590/fst.81421.

[11] D. Gómez, E. Azón, N. Marco, J.J. Carramiñana, C. Rota, A. Ariño, J. Yangüela, Antimicrobial resistance of *Listeria monocytogenes* and *Listeria innocua* from meat products and meat-processing environment, Food Microbiol. 42 (2014) 61–65, https://doi.org/10.1016/j.fm.2014.02.017.

[12] R. Orsi, M. Wiedmann, Characteristics and distribution of *Listeria* spp., including *Listeria* species newly described since 2009, Appl. Microbiol. Biotechnol. 100 (2016) 5273–5287, https://doi.org/10.1007/s00253-016-7552-2.

[13] R. Campana, L. Casettari, L. Fagioli, M. Cespi, G. Bonacucina, W. Baffone, Activity of essential oil-based microemulsions against *Staphylococcus aureus* biofilms on stainless steel surface in different culture media and growth conditions, Int. J. Food Microbiol. 241 (2017) 132–140, https://doi.org/10.1016/j.ijfoodmicro.2016.10.021.

[14] J. Yammine, N.E. Chihib, A. Gharsallaoui, E. Dumas, A. Ismail, L. Karam, Essential oils and their active components applied as: free, encapsulated and in hurdle technology to fight microbial contaminations. A review, Heliyon 8 (2022), e12472, https://doi.org/10.1016/j.heliyon.2022.e12472.

[15] M. Sharifi-Rad, E.M. Varoni, M. Iriti, M. Martorell, W.N. Setzer, M. del Mar Contreras, B. Salehi, A. Soltani-Nejad, S. Rajabi, M. Tajbakhsh, J. Sharifi-Rad, Carvacrol and human health: a comprehensive review: carvacrol and human health, Phytother Res. 32 (2018) 1675–1687, https://doi.org/10.1002/ptr.6103.

[16] A.T. Bernal-Mercado, J. Juarez, M.A. Valdez, J.F. Ayala-Zavala, C.L. Del-Toro-Sánchez, D. Encinas-Basurto, Hydrophobic chitosan nanoparticles loaded with carvacrol against *Pseudomonas aeruginosa* biofilms, Molecules 27 (2022), https://doi.org/10.3390/molecules27030699. Article 699.

[17] A. De Abreu Pereira, J. Pamplona Pagnossa, J. Paulo Alcântara, S. Rodrigo Isidoro, R. Hilsdorf Piccoli, Interaction of *Salmonella* sp. and essential oils: bactericidal activity and adaptation capacity, Science and Technology Journal 12 (2019) 1–6, https://doi.org/10.18779/cyt.v12i2.320.

[18] J.B. Engel, C. Heckler, E.C. Tondo, D.J. Daroit, P. da Silva Malheiros, Antimicrobial activity of free and liposome-encapsulated thymol and carvacrol against *Salmonella* and *Staphylococcus aureus* adhered to stainless steel, Int. J. Food Microbiol. 252 (2017) 18–23, https://doi.org/10.1016/j.ijfoodmicro.2017.04.003.

[19] C. Heckler, C. Marques Maders Silva, F. Ayres Cacciatore, D.J. Daroit, P. da Silva Malheiros, Thymol and carvacrol in nanoliposomes: characterization and a comparison with free counterparts against planktonic and glass-adhered *Salmonella*, Lebensm. Wiss. Technol. 127 (2020), https://doi.org/10.1016/j.lwt.2020.109382. Article 109382.

[20] A. Nair, R. Mallya, V. Suvarna, T.A. Khan, M. Momin, A. Omri, Nanoparticles—attractive carriers of antimicrobial essential oils, Antibiotics 11 (2022), https://doi.org/10.3390/antibiotics11010108. Article 108.

[21] C. Sahli, S.E. Moya, J.S. Lomas, C. Gravier-Pelletier, R. Briandet, M. Hémadi, Recent advances in nanotechnology for eradicating bacterial biofilm, Theranostics 12 (2022) 2383–2405, https://doi.org/10.7150/thno.67296.

[22] R.V. de Barros Fernandes, S.V. Borges, E.K. Silva, Y.F. da Silva, H.J.B. de Souza, E. L. do Carmo, C.R. de Oliveira, M.I. Yoshida, D.A. Botrel, Study of ultrasound-assisted emulsions on microencapsulation of ginger essential oil by spray drying, Ind. Crop. Prod. 94 (2016) 413–423, https://doi.org/10.1016/j.indcrop.2016.09.010.

[23] T.T.T. Nguyen, T.V.A. Le, N.N. Dang, D.C. Ngyuyen, P.T.N. Nguyen, T.T. Tran, Q. V. Nguyen, L.G. Bach, T.D. Pham, Microencapsulation of essential oils by spray-drying and influencing factors, J. Food Qual. 2021 (2021) 1–15, https://doi.org/10.1155/2021/5525879.

[24] H. Chen, Y. Zhang, Q. Zhong, Physical and antimicrobial properties of spray-dried zein–casein nanocapsules with co-encapsulated eugenol and thymol, J. Food Eng. 144 (2015) 93–102, https://doi.org/10.1016/j.jfoodeng.2014.07.021.

[25] M. Luna, O. Beltran, D.A. Encinas-Basurto, M.G. Ballesteros-Monrreal, A. Topete, N. Hassan, M.A. Lopez-Mata, V. Reyes-Marquez, M.A. Valdez, Josué Juarez, High antibacterial performance of hydrophobic chitosan-based nanoparticles loaded with carvacrol, Colloids Surf. B Biointerfaces 209 (2022), 112191, https://doi.org/10.1016/j.colsurfb.2021.112191.

[26] M.V.O.B. Maciel, C.G. da Rosa, A.R. Almeida, M.R. Nunes, C.M. Noronha, B. Jummes, S.M. Martelli, F.C. Bertoldi, P.L.M. Barreto, Thymol loaded zein microparticles obtained by spray-drying: physical-Chemical Characterization, Biocatal. Agric. Biotechnol. 37 (2021), https://doi.org/10.1016/j.bcab.2021.102177. Article 102177.

[27] M. Mondéjar-Lopez, A.J. Lopez-Jimenez, J.C. Garcia Martinez, O. Ahrazem, L. Gomez-Gomez, E. Niza, Comparative evaluation of carvacrol and eugenol chitosan nanoparticles as eco-friendly preservative agents in cosmetics, Int. J. Biol. Macromol. 206 (2022) 288–297, https://doi.org/10.1016/j.ijbiomac.2022.02.164.

[28] T. Wang, J. Xue, Q. Hu, M. Zhou, Y. Luo, Preparation of lipid nanoparticles with high loading capacity and exceptional gastrointestinal stability for potential oral delivery applications, J. Colloid Interface Sci. 507 (2017) 119–130, https://doi.org/10.1016/j.jcis.2017.07.090.

[29] C. Dima, L. Patrascu, A. Cantaragiu, P. Alexe, S. Dima, The kinetics of the swelling process and the release mechanisms of *Coriandrum sativum* L. essential oil from chitosan/alginate/inulin microcapsules, Food Chem. 195 (2016) 39–48, https://doi.org/10.1016/j.foodchem.2015.05.044.

[30] E. Lainez-Cerón, N. Ramirez-Corona, A. Lopez-Malo, A. Franco-Vega, An overview of mathematical modeling for conventional and intensified processes for extracting essential oils, Chemical Engineering and Processing - Process Intensification 178 (2022), 109032, https://doi.org/10.1016/j.cep.2022.109032.

[31] F. Teshale, K. Narendiran, S.M. Beyan, N.R. Srinivasan, Extraction of essential oil from rosemary leaves: optimization by response surface methodology and mathematical modeling, Applied Food Research 2 (2022), 100133, https://doi.org/10.1016/j.afres.2022.100133.

[32] Y. Premjit, S. Pandey, J. Mitra, Recent trends in folic acid (vitamin B9) encapsulation, controlled release, and mathematical modelling, Food Rev. Int. 17 (2022) 1–35, https://doi.org/10.1080/87559129.2022.2077361.

[33] A. Shetta, J. Kegere, W. Mamdouh, Comparative study of encapsulated peppermint and green tea essential oils in chitosan nanoparticles: encapsulation, thermal stability, in-vitro release, antioxidant and antibacterial activities, Int. J. Biol. Macromol. 126 (2019) 731–742, https://doi.org/10.1016/j.ijbiomac.2018.12.161.

[34] M. Abdallah, O. Khelissa, A. Ibrahim, C. Benoliel, L. Heliot, P. Dhulster, N. E. Chihib, Impact of growth temperature and surface type on the resistance of *Pseudomonas aeruginosa* and *Staphylococcus aureus* biofilms to disinfectants, Int. J. Food Microbiol. 214 (2015) 38–47, https://doi.org/10.1016/j.ijfoodmicro.2015.07.022.

[35] M. Kord Heydari, E. Assadpour, S.M. Jafari, H. Javadian, Encapsulation of rose essential oil using whey protein concentrate-pectin nanocomplexes: optimization of the effective parameters, Food Chem. 356 (2021), https://doi.org/10.1016/j.foodchem.2021.129731. Article 129731.

[36] A.G.B. Dantas, R.L. de Souza, A.R. de Almeida, F.H. Xavier Júnior, M.G.D.R. Pitta, M.j. b. d. m. Rêgo, E.E. Oliveira, Development, characterization, and immunomodulatory evaluation of carvacrol-loaded nanoemulsion, Molecules 26 (2021) 3899, https://doi.org/10.3390/molecules26133899.

[37] S. Beirão-da-Costa, C. Duarte, A.I. Bourbon, A.C. Pinheiro, M.I.N. Januário, A. A. Vicente, M.L. Beirão-da-Costa, I. Delgadillo, Inulin potential for encapsulation and controlled delivery of Oregano essential oil, Food Hydrocolloids 33 (2013) 199–206, https://doi.org/10.1016/j.foodhyd.2013.03.009.

[38] M. Mehran, S. Masoum, M. Memarzadeh, Microencapsulation of Mentha spicata essential oil by spray drying: optimization, characterization, release kinetics of essential oil from microcapsules in food models, Ind. Crop. Prod. 154 (2020), https://doi.org/10.1016/j.indcrop.2020.112694. Article 112694.

[39] W. Li, W. Li, Y. Wan, L. Wang, T. Zhou, Preparation, characterization and releasing property of antibacterial nano-capsules composed of ε-PL-EGCG and sodium

alginate-chitosan, Int. J. Biol. Macromol. 204 (2022) 652–660, https://doi.org/10.1016/j.ijbiomac.2022.01.123.
[40] E. Ercin, S. Kecel-Gunduz, B. Gok, T. Aydin, Y. Budama-Kilinc, M. Kartal, Laurus nobilis L. essential oil-loaded PLGA as a nanoformulation candidate for cancer treatment, Molecules 27 (2022), https://doi.org/10.3390/molecules27061899. Article 1899.
[41] S. Das, V.K. Singh, A.K. Chaudhari, A.K. Dwivedy, N.K. Dubey, Co-encapsulation of Pimpinella anisum and Coriandrum sativum essential oils based synergistic formulation through binary mixture: physico-chemical characterization, appraisal of antifungal mechanism of action, and application as natural food preservative, Pestic. Biochem. Physiol. 184 (2022), https://doi.org/10.1016/j.pestbp.2022.105066. Article 105066.
[42] T. Tyagi, P.K. Garlapati, P. Yadav, M. Naika, A. Mallya, A. Kandangath Raghavan, Development of nano-encapsulated green tea catechins: studies on optimization, characterization, release dynamics, and in-vitro toxicity, J. Food Biochem. 45 (2021), e13951, https://doi.org/10.1111/jfbc.13951.
[43] S.L. Pal, U. Jana, P.K. Manna, G.P. Mohanta, R. Manavalan, Nanoparticle: an overview of preparation and characterization, J. Appl. Pharmaceut. Sci. 1 (2011) 228–234, https://doi.org/10.7897/2230-8407.04408.
[44] C. Cai, R. Ma, M. Duan, D. Lu, Preparation and antimicrobial activity of thyme essential oil microcapsules prepared with gum Arabic, RSC Adv. 9 (2019) 19740–19747, https://doi.org/10.1039/C9RA03323H.
[45] A. Guarda, J.F. Rubilar, J. Miltz, M.J. Galotto, The antimicrobial activity of microencapsulated thymol and carvacrol, Int. J. Food Microbiol. 146 (2011) 144–150, https://doi.org/10.1016/j.ijfoodmicro.2011.02.011.
[46] M. Sotelo-Boyás, Z. Correa-Pacheco, S. Bautista-Baños, Y. Gómez y Gómez, Release study and inhibitory activity of thyme essential oil-loaded chitosan nanoparticles and nanocapsules against foodborne bacteria, Int. J. Biol. Macromol. 103 (2017) 409–414, https://doi.org/10.1016/j.ijbiomac.2017.05.063.
[47] J. Bajac, B. Nikolovski, I. Lončarević, J. Petrović, B. Bajac, S. Đurović, L. Petrović, Microencapsulation of juniper berry essential oil (Juniperus communis L.) by spray drying: microcapsule characterization and release kinetics of the oil, Food Hydrocolloids 125 (2022), https://doi.org/10.1016/j.foodhyd.2021.107430. Article 107430.
[48] E.D. Herculano, H.C.B. de Paula, E.A.T. de Figueiredo, F.G.B. Dias, V. de A. Pereira, Physicochemical and antimicrobial properties of nanoencapsulated Eucalyptus staigeriana essential oil, LWT - Food Sci. Technol. (Lebensmittel-Wissenschaft -Technol.) 61 (2015) 484–491, https://doi.org/10.1016/j.lwt.2014.12.001.
[49] A. Gonçalves, B.N. Estevinho, F. Rocha, Spray-drying of oil-in-water emulsions for encapsulation of retinoic acid: polysaccharide- and protein-based microparticles characterization and controlled release studies, Food Hydrocolloids 124 (2022), https://doi.org/10.1016/j.foodhyd.2021.107193. Article 107193.
[50] A.G. de Souza, R.F.S. Barbosa, Y.M. Quispe, D.S. Rosa, Essential oil microencapsulation with biodegradable polymer for food packaging application, J. Polym. Environ. 3 (2022) 1–9, https://doi.org/10.1007/s10924-022-02436-y.
[51] R.F.S. Barbosa, E.D.C. Yudice, S.K. Mitra, D.S. Rosa, Characterization of Rosewood and Cinnamon Cassia essential oil polymeric capsules: stability, loading efficiency, release rate and antimicrobial properties, Food Control 121 (2021), https://doi.org/10.1016/j.foodcont.2020.107605. Article 107605.
[52] W. Low, M.A. Kenward, M. Amin, C. Martin, Ionically crosslinked chitosan hydrogels for the controlled release of antimicrobial essential oils and metal ions for wound management applications, Medicines 3 (2016), https://doi.org/10.3390/medicines3010008. Article 8.
[53] L.C. Silva, R.M. Castelo, H.C.R. Magalhães, R.F. Furtado, H.N. Cheng, A. Biswas, C. R. Alves, Characterization and controlled release of pequi oil microcapsules for yogurt application, Lebensm. Wiss. Technol. 157 (2022), https://doi.org/10.1016/j.lwt.2022.113105. Article 113105.
[54] P. Jin, R. Yao, D. Qin, Q. Chen, Q. Du, Enhancement in antibacterial activities of eugenol-entrapped ethosome nanoparticles via strengthening its permeability and sustained release, J. Agric. Food Chem. 67 (2019) 1371–1380, https://doi.org/10.1021/acs.jafc.8b06278.
[55] J. Hu, Y. Zhang, Z. Xiao, X. Wang, Preparation and properties of cinnamon-thyme-ginger composite essential oil nanocapsules, Ind. Crop. Prod. 122 (2018) 85–92, https://doi.org/10.1016/j.indcrop.2018.05.058.
[56] D. Pérez-Conesa, J. Cao, L. Chen, L. McLandsborough, J. Weiss, Inactivation of *Listeria monocytogenes* and *Escherichia coli* O157:H7 biofilms by micelle-encapsulated eugenol and carvacrol, J. Food Protect. 74 (2011) 55–62, https://doi.org/10.4315/0362-028X.JFP-08-403.